

Sensitivity study of cloud-resolving convective simulations with WRF using the PLIN and WSM6 microphysical parameterizations

Song-You Hong, Kyo-Sun Lim, Ju-Hye Kim, Jeong-Ock Jade Lim, and Jimy Dudhia*

Department of Atmospheric Sciences, Yonsei University, Seoul, Korea

*Mesoscale and Microscale Meteorology Division/National Center for Atmospheric Research, Boulder, Colorado, USA

1. Introduction

At NCAR, real time forecasting experiments with a 4-km grid mesh over the central US employed the WRF-Single-Moment 6class (WSM6) Microphysics scheme that replaced the Purdue Lin (PLIN) scheme in early 2005. Both schemes have the same number of prognostic water substance including graupel. Although some preliminary reports identified the overall superiority of the WSM6 to the PLIN scheme in resolving precipitating convective systems (e.g., Klemp 2006, Kuo 2006), reasons for the different behaviors have not been clarified.

The goal of this research is to understand the importance of microphysics, especially ice-phase microphysics processes in the bulk parameterization. The performance of the WSM6 microphysics will be evaluated, compared to that of the PLIN scheme, focusing on the major differences in the treatment of ice properties and their sedimentation velocity. Section 2 provides overall differences between the WSM6 and PLIN schemes. In section 3, the numerical experiments conducted in this study are described, with their results being discussed in section 4. Concluding remarks appear in the final section.

2. Comparison of the WSM6 and PLIN schemes

The most important difference in the two schemes is the treatment of ice-phase microphysical processes (Table 1). The WSM6 scheme treats the ice crystal number concentration (N_I) as a function of cloud ice amount (ρq_I), and the ice nuclei number concentration (N_{I0}) is separated from N_I , whereas the PLIN scheme uses the formula of Fletcher (1962) for both N_I and N_{I0} . Related changes for the ice-phase microphysics are described in HDC. In addition to the distinguishing differences in ice-microphysics devised by Hong et al. (2004), the production and generation terms for the water substances in the two schemes differ.

Another apparent difference is the treatment of the snow and graupel sedimentation. As in Hong and Lim (2006), the mass weighted terminal

velocity for graupel in the WSM6 scheme, V_G , is given by

$$V_G [\text{m s}^{-1}] = \frac{a_G \Gamma (4 + b_G)}{6} \left(\frac{\rho_o}{\rho} \right)^{\frac{1}{2}} \frac{1}{\lambda_G^{b_G}} \quad (1)$$

where a_G and b_G are the empirical coefficients for terminal velocity, λ_G the slope parameter, ρ the density of air, and ρ_o the density of air at reference state. The PLIN scheme also employs the same formula, but the different coefficients, a_G and b_G (see Table 1). It is seen that the mass weighted terminal velocity for graupel, V_G , is about twice as fast in the PLIN scheme than in the WSM6 scheme. The terminal velocity for snow, V_S , is also different, but not significantly. Thus, major differences in the WSM6 and PLIN schemes can be categorized by the 1) ice-phase microphysics based on HDC and 2) terminal velocity for graupel. The relative importance of the two components in the WSM6 and PLIN schemes will be investigated.

Table 1. Major differences of the microphysics parameterization between the WSM6 and PLIN schemes

	WSM6	PLIN
Ice number concentration, N_I (m^{-3})	$5.38 \times 10^7 (\rho q_I)^{0.75}$	$10^3 \exp[0.5(T_0 - T)]$
Ice nuclei number, N_{I0} (m^{-3})	$10^3 \exp[0.1(T_0 - T)]$	$10^2 \exp[0.5(T_0 - T)]$
Snow intercept parameter, n_{0S} (m^{-4})	$2 \times 10^6 \exp[0.12(T_0 - T)]$	3×10^6
Density of graupel, ρ_G (kg m^{-3})	500	400
Constant a_G	330	82.5
Constant b_G	0.8	0.5

3. Numerical Experimental Setup

The model used in this study is the Advanced Research WRF version 2.1.2. Two sets of experiments were carried out: an idealized 2D thunderstorm case and a 3D real-data simulation of a heavy rainfall event over Korea. The 2D idealized thunderstorm experiment was designed to

systematically distinguish the intrinsic differences between the WSM6 and PLIN schemes by the virtue of fixed initial conditions and the absence of other non-microphysical processes, which in turn would help us to understand the impact of the changes in the microphysics in the 3D framework. The second test case was a real-data example for 24 h, ending at 0000 UTC July 15, 2001.

In addition to the WSM6 and PLIN experiments, another set of sensitivity experiment is carried out to determine the relative importance of two factors in the scheme as mentioned above. The WSM6_v_g (PLIN_v_g) experiment replacing the v_g in the WSM6 (PLIN) scheme by that in the PLIN (WSM6) scheme, is designed to identify a major difference between the WSM6 and PLIN schemes. An additional experiment, WSM6_nora, that excludes the effects of clouds on the radiation computation, is designed to further investigate the ice-cloud/radiation feedback.

4. Results and discussion

a. Idealized experiments

The time series of domain-averaged precipitation and hydrometeor path is plotted in Fig. 1. It can be seen that the WSM6 scheme develops the mature stage of the storm about 10 min later, as compared to the PLIN scheme, although initial development before 25 min is as fast (Fig. 1a). The maximum intensity of precipitation is also weakened in the WSM6 experiment. Meanwhile, the results from the WSM6_v_g and PLIN_v_g experiments identify that both the evolution of surface precipitation and hydrometeors are significantly affected by the magnitude of sedimentation of graupel, rather than differences in the ice-phase microphysics.

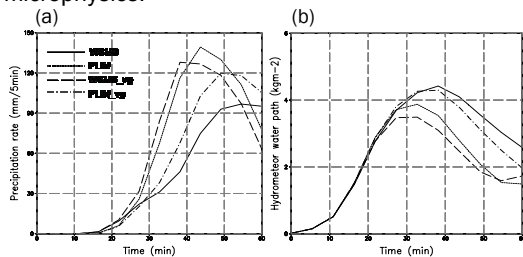


Fig. 1. Time series of the (a) surface precipitation rate, and (b) hydrometeor path amount averaged over the domain, resulted from the WSM6 (solid), PLIN (dotted), WSM6_v_g (dashed), and PLIN_v_g (dot-dashed) experiments.

The immediate impact of the different sedimentation velocity would appear in the distribution of hydrometeors (Fig. 2a). Compared to the results from the WSM6 run, the reduction of graupel above the freezing level with the maximum at 8 km is evident in the WSM6_v_g run. The reduction of other hydrometeors is not as distinct as in the graupel, but still visible, and can be attributed to enhanced accretion of them by graupel.

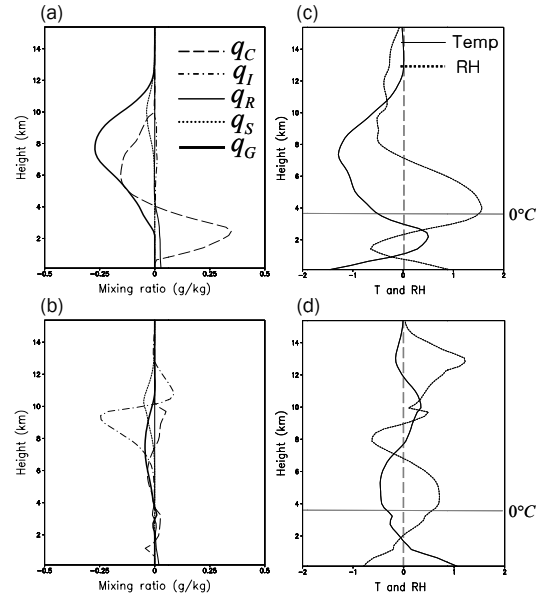


Fig. 2. Differences in the vertical profiles of (a) hydrometeors (Units are gkg^{-1} for rain, snow, and graupel, and 10gkg^{-1} for cloud ice and cloud waters.), and (c) temperature and relative humidity (WSM6_v_g minus WSM6), and (b), (d) for the differences of PLIN_v_g and WSM6 experiment (PLIN_v_g minus WSM6). Units are 0.1°C for temperature (Temp) and % for relative humidity (RH). All fields are obtained from domain-averaged during the 60 min integration period.

A detailed analysis of each source/sink term in the WSM6 scheme identified that the accretion process of cloud water by graupel (Pgacw) is the dominant process for graupel formation in the convective system when the temperature is below 0°C , consistent with the results of Wang et al. (2007). Thus, a relative cooling above the freezing level in the case of the WSM6_v_g run (Fig. 2c) can be attributed to the reduction of latent heat release from freezing in the Pgacw term at the later stages of storm development because of the reduced graupel aloft. Analysis also shows that given the same amount of mass flux, the faster sedimentation of graupel enhances melting and sublimation as well as accretion of other hydrometeors since graupel is carried to lower levels more rapidly, which results in the reduction of hydrometeors aloft. The increase of cloud water below the freezing level may be due to the fact that increased surface cooling and enhanced surface rainfall from more rain increase the gust-front lifting to produce more clouds and condensation (Fig. 2a).

Compared to the impact of the sedimentation velocity for graupel, differences in the ice-phase microphysics between the WSM6 and PLIN schemes do not affect significantly the storm evolution in this idealized test framework (compare Figs. 2a and 2b, Figs. 2c and 2d). Compared to the WSM6 physics, the increase of cloud ice at colder temperatures (~ 11 km) and its reduction at warmer temperatures (~ 9 km) are prominent in the PLIN physics run, together with the reduction of snow

amount (Fig. 2b), which reflects the typical characteristics of HDC ice-phase microphysics. The decrease of graupel can be attributed to the weakening of accretion due to the reduced amount of ice and snow. The enhanced heating with the maximum at 10 km perhaps reflects the increase of liquid hydrometeors at that height in the PLIN physics, whereas the decrease of them below that level may be related to relative cooling and moistening due to less cloud water to be frozen and the saturation profile of PLIN that is weighted by ice and water content (Fig. 2d).

From Figs. 1 and 2, it is found that the impact of the sedimentation velocity for graupel overwhelms the effect of microphysics on the storm evolution in terms of precipitation intensity. A relatively short integration time in the 2D run could be a reason why the impact of ice-phase microphysics is relatively insignificant. Recognizing the limitations of the comparison results in the 2D idealized run, the relative importance of the ice-microphysics and sedimentation velocity for graupel is different in the case of the 3D simulation, as will be shown in the following sub-section.

b. Heavy rainfall (snowfall) event

Figure 3 compares the predicted 24-h accumulated rain valid at 00 UTC 15 July 2001. More precipitation is simulated by the PLIN than by the WSM6 scheme and this results in the deterioration of the bias score for precipitation. Another distinct impact is that compared to the results from the PLIN experiment, the WSM6 scheme shifts the major precipitation band southward towards what was observed, leading to the improved pattern correlation in the case of the WSM6 run. In the WSM6 experiment, coexisting ice and snow are seen at warmer temperatures below 400 mb, whereas there is negligible ice at these levels in the PLIN experiment (not shown).

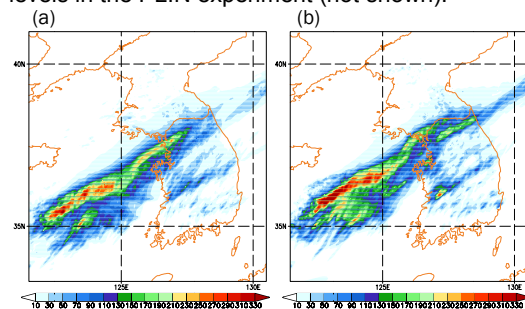


Fig. 3. 24-hr accumulated rainfall (mm) ending at 0000 UTC 15 July 2001, from the 3-km resolution experiments with the (a) WSM6 and (b) PLIN schemes

The impact of the sedimentation velocity for graupel is quite different from the results that are obtained in the 2D run. It is clear that the evolution of domain-averaged precipitation from the WSM6_vg run (PLIN_vg) is very close to that with the WSM6 (PLIN) experiment (cf. Fig. 4a and Fig.

1a), whereas the evolution of volume-averaged water substances in the WSM6_vg (PLIN_vg) experiment follows the impact as shown in the 2D idealized experiment (cf. Fig. 4b and Fig. 1b). The horizontal distribution of precipitation also confirmed that the northward (south) shifting of precipitation band, as seen in Fig. 3, also appears in the PLIN_vg (WSM6_vg) run (not shown). A possible reason for the different sensitivity is given below.

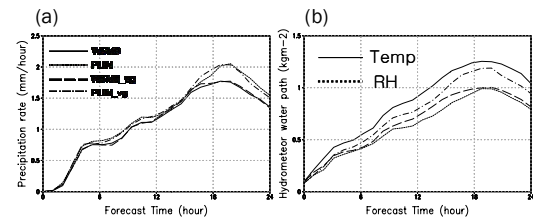


Fig. 4. Time series of the (a) precipitation rate (b) hydrometeor water path, resulted from the WSM6 (solid), PLIN (dotted), WSM6_vg (dashed), and PLIN_vg (dot-dashed) experiments at the 3-km resolution, averaged over the heavy rainfall region (33.3-41.0 N, 121.5-130.5 E).

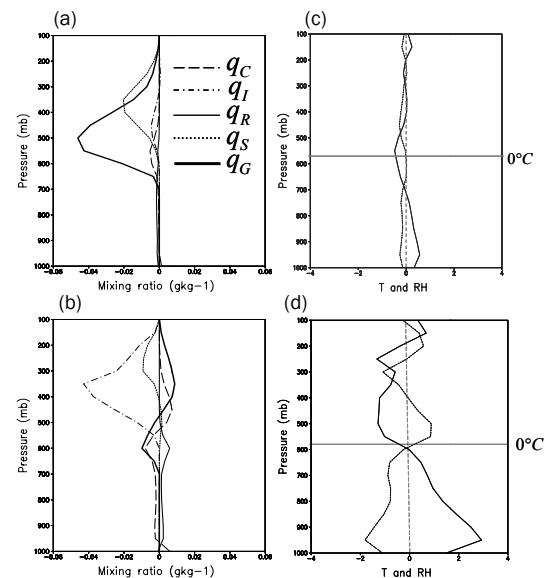


Fig. 5. Same as in Fig. 2, but for the heavy rainfall experiments at the 3-km resolution, averaged over the heavy rainfall region (33.3-41.0 N, 121.5-130.5 E).

The vertical profiles of the differences in hydrometeors generally follow the characteristics seen in the 2D run. Differences in vertical distribution of graupel due to the different microphysics are also similar to that seen in the 2D run, but there is a relatively large reduction of graupel in the upper troposphere when the WSM6 physics is employed. A major difference is found in the distribution of liquid phase hydrometeors. The amount of surface rainfall from the WSM6_vg run is very similar to that from the WSM6 run, which is different from the results in the 2D case (Fig. 2a and Fig. 5a). Also, the increase of cloud water in the WSM6_vg run seen in the 2D run is not distinct

in the 3D run. The corresponding differences in temperature, and specific humidity are not directly explainable in this 3D run framework, but it is distinct that the changes due to the microphysics are larger than those due to the sedimentation velocity (c.p. Fig. 5c and 5d).

A reason for the different effect between the 2D and 3D runs can be deduced from the different thermodynamic environments. In the model relative humidity is a variable for evaporation with the assumption that modeled raindrops are assumed to be at the same temperature as the air. For example, in the 2D case, layers around the freezing level are nearly saturated because of strong updrafts, so that the melting process is more efficient than the evaporation of the graupel, and vice versa due to lower relative humidity in the 3D case.

Another reason can be deduced from the interaction between the ice clouds and radiation. The reduction of ice particles through faster sedimentation of graupel in the WSM6_{v_g} run increases short-wave radiation reaching the surface, which results in warming the lower troposphere (Fig. 5c). The reduction of cloud ice in the PLIN physics also brings about the increase of solar radiation at the surface (Fig. 5d). As a result, the decrease of the stability within the entire troposphere in the PLIN scheme provides a favorable environment for convective activity. Both effects enhance the buoyancy for triggering convection, leading to enhanced rainfall at the surface, but with a larger impact by the ice-phase microphysics than by the fall velocity. This may be due to that fact that ice cloud has a stronger cloud/radiation feedback than other ice particles since areal coverage for ice is relatively large.

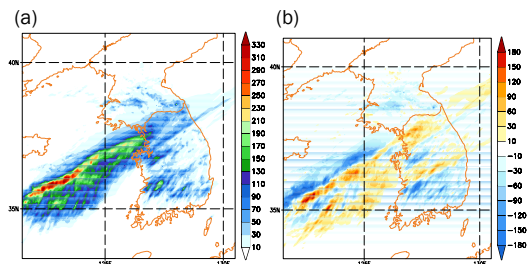


Fig. 6. The 24-hr accumulated rainfall (mm) ending at 00 UTC 15 July 2001, from the (a) WSM6_{nora} experiment and the (b) difference (WSM6 minus WSM6_{nora}).

To further confirm the role of the revised ice-microphysics in the WSM6 scheme, another sensitivity experiment that excludes the cloud-radiation feedback is conducted. In Fig. 6, it is seen that the WSM6 scheme without the cloud-radiation feedback shifts the major rain band northward, which is the same way as was simulated by the PLIN scheme. By comparing the three results from the WSM6, PLIN, and WSM6 without radiation feedback experiments, it can be deduced that the southward displacement of the simulated precipitation in the WSM6 scheme, as compared to

that from the PLIN scheme, is due to the enhanced ice cloud amounts and their radiation feedback. These are further explained below.

Increased ice cloud above leads to the reduced longwave cooling in the upper troposphere, which shows as a relative warming effect below 200 mb. Cooling above 200 mb is also enhanced due to the increased longwave cloud-top effect. Additionally, the decrease of downward solar energy induces a cooling near the surface. This stabilization effect appears broadly from south to north across the precipitation band. Thus, the air to the north has less chance for forming clouds since temperature is colder and relative humidity is drier with latitude. The air to the south is still buoyant, although the surface is cooler. As a result, the WSM6 scheme tends to stabilize the atmosphere, as compared to the PLIN scheme, which enhances (suppresses) vertical motion to the south (north). This effect is smaller in the comparison of the WSM6 and PLIN schemes, but still visible. Due to a reduced amount of ice-clouds in the PLIN scheme, the cloud-radiation feedback would be weakened in the PLIN scheme, and consequently, the WSM6 scheme displaces the rainband south through an enhanced feedback between clouds and radiation processes.

5. Concluding remarks

This study provides the relative importance of ice-phase microphysics and fall velocity for ice particles in the bulk-type parameterization approach of clouds and precipitation, and sheds some light on the clouds and radiation interaction in forming precipitating convection. Comparing WSM6 with PLIN, also implies that the impact of the complexity in the microphysics due to the number of prognostic water substance variables on simulated convective activity is smaller than the effects of the manner in which each microphysical process is formulated in the same category of prognostic water substance variables.

Finally, it is important to note that the bulk schemes being compared were the WSM6 and PLIN schemes within WRF which are relatively similar bulk schemes, indicating that the findings of this research are specific to these schemes. Despite such a restriction, our findings for the relative role in ice-phase microphysics and its sedimentation velocity are certainly useful.

The content of this paper is based on the study of Hong et al. (2008, *J. Applied Meteorology and Climatology*, in review), and the new unified velocity proposed in this study was announced in WRF version 3.0.

Acknowledgements

This research was supported by the Korean Foundation for International Cooperation of Science & Technology (KICOS) through a grant provided by the Korean Ministry of Science & Technology (MOST) in 2007.